Nanoparticle and Process Induced Super Toughened Piezoelectric Hybrid Materials: The Effect of Stretching on Filled System

ARTICLE *in* MACROMOLECULES · JULY 2013

Impact Factor: 5.8 · DOI: 10.1021/ma400603h

Macromolecules

Article

pubs.acs.org/Macromolecules

Nanoparticle and Process Induced Super Toughened Piezoelectric Hybrid Materials: The Effect of Stretching on Filled System

Vimal K. Tiwari,[†] Amit K. Prasad,[†] Vaishali Singh,[†] Karun K. Jana,[†] Manjusri Misra,[‡] C. Durga Prasad,[§] and Pralay Maiti*,[†]

[†]School of Materials Science and Technology, Indian Institute of Technology (Banaras Hindu University), Varanasi 221 005, India

[‡]School of Engineering and the Department of Plant Agriculture, Thombrough Building, University of Guelph, Guelph, Ontario N1G 2W1, Canada

[§]Naval Materials Research Laboratory (NMRL), Ambernath, Thane 421 506, India

Supporting Information

ABSTRACT: Process and nanoparticle induced piezoelectric super toughened poly(vinylidene fluoride) (PVDF) nanohybrids have been demonstrated. The nanohybrids have been prepared by incorporating organically modified nanoclay through melt extrusion and solution route. The solution processed nanohybrid exhibit 1100% improvement in toughness as well as adequate stiffness as compared to pure PVDF without any trade-off. The structural and morphological origins of super toughening phenomena have been worked out. The unique crystallization behavior of PVDF on top of the silicate layers (β-phase, planar zigzag chain conformation, and subsequent polar γ-phase and α-phase as layered type) has been revealed to create an island type of structure, which in turn is responsible for greater toughness. The extent of piezoelectric β-phase has been enhanced by controlled stretching of the nanohybrid at moderately high temperature for better disentanglement, and 90% of the piezoelectric phase has been stabilized. The structural change over has been confirmed through XRD, FTIR, and DSC studies. The nanohybrids possess β-phase with a small amount of α-phase and distorted γ-phase (T_3G-T_6G) before stretching which convert into predominantly β-phase with increasing the draw ratio, whereas pure PVDF converted directly into β-phase from pure α-phase. The piezoelectric coefficient (d_{33}) exhibits significant increase with draw ratio, and the relative enhancement is more in nanohybrid vis-à-vis pure PVDF arising from the presence of greater β-phase leading to super toughened lightweight piezoelectric material.

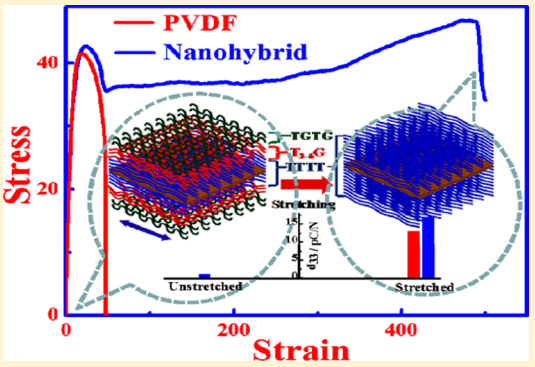

1. INTRODUCTION

Poly(vinylidene fluoride) (PVDF) exhibits many important properties, such as mechanically strong, high temperature and chemically resistant, UV and nuclear radiation resistance, high abrasion and aging resistance, and piezo- and pyroelectric, and has applications in versatile technological importance including sensors and actuators.[1,2] Moreover, it has significant medical applications[3] because of its nonrejectable nature in human tissues. PVDF, a highly nonreactive thermoplastics, is intriguing because of its availability in different crystalline forms having three modes of molecular conformations, $TGT\bar{G}$, $TTTT$, and $TTTGTTT\bar{G}$, and crystallizes in five types of crystalline modifications distinguished as α, β, γ, δ, and ε forms.[4] The nonpolar α-phase (form II) is the thermodynamically stable phase having $TGT\bar{G}$ conformation. The β-phase (form I, metastable state) is responsible for piezo- and pyroelectric properties having all-trans ($TTTT$) conformation.[5,6] The β-form can usually be obtained from melt crystallization at high pressure,[7] polling at high voltage,[8] stretching, recrystallization on carbon-coated highly oriented ultrathin film,[9,10] and molecular epitaxy on the surface of potassium bromide.[11] Possibility of form III was suggested on the basis of IR spectra, and subsequently the form III was prepared at high pressure crystallization by Doll and Lando with a melting point 15 °C above the melting temperature of α- and β-phases[12] with characteristic IR peaks at 430, 776, 810, and 1234 cm^{-1}.[13] First report of the stabilization of β-phase PVDF, in the presence of organically modified nanoclay through melt intercalation,[14] shows increase in stiffness from 1.3 to 1.8 GPa, whereas increment in elongation at break and enhancement in toughness were reported to be 140% and 700% higher than those of pure PVDF, respectively.[15] Significant improvement in toughness for the copolymer P(VDF−CTFE) is reported through enhanced specific surface area, better mechanical interlocking/adhesion at the interface of nanofiller, and more polar chloro-substituted fluoropolymer.[16] In the presence of other nanofillers like CNT and graphene, nanohybrids of PVDF show lower elongation and toughness with higher

Received: March 23, 2013
Revised: June 25, 2013
Published: July 9, 2013

   dx.doi.org/10.1021/ma400603h | Macromolecules 2013, 46, 5595−5603

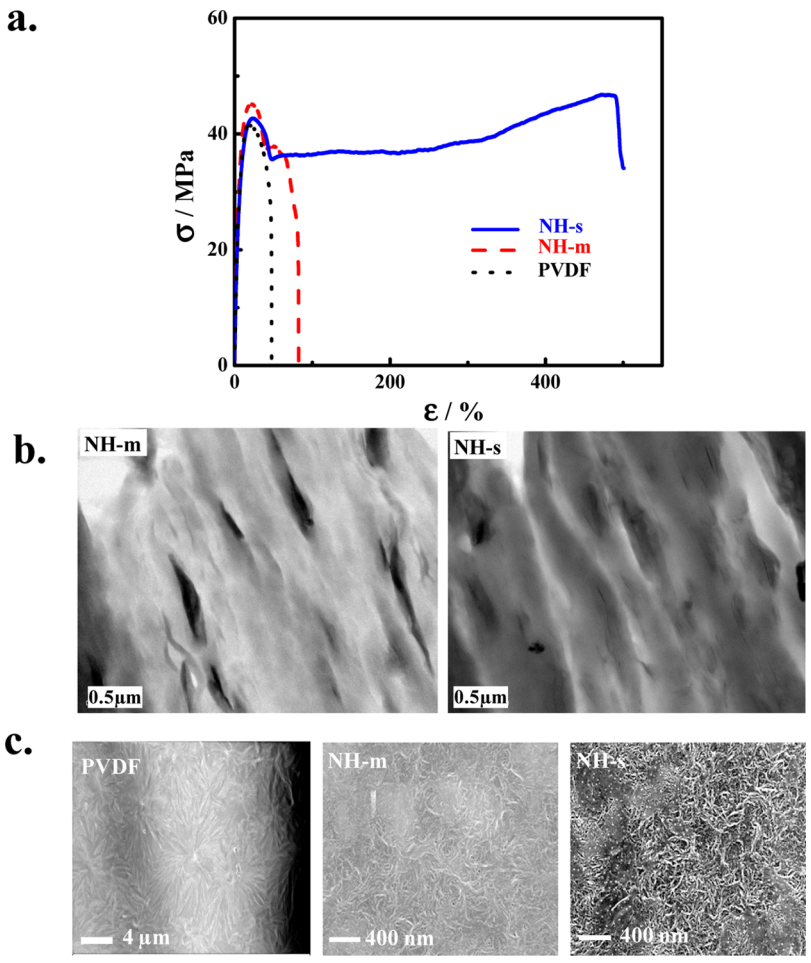

Figure 1. Super toughening phenomena. (a) Stress–strain curves of pure PVDF, nanohybrid melt (NH-m), and nanohybrid sol (NH-s), NH-s showing the dramatic increase in elongation at break. (b) Bright field TEM images of PVDF nanohybrid processed through melt (NH-m) and solution route (NH-s). (c) SEM images of pure PVDF, PVDF nanohybrid melt (NH-m), and solution casting (NH-s).

modulus due to insufficient interaction between the fillers and polymer.[17,18] The blend of poly(vinylidene fluoride) (PVDF)/poly(methyl methacrylate) (PMMA) provides flat ferroelectric film with nanometer scale β-type PVDF crystals based on spin-coating and subsequent melt-quenching.[19,20] A much higher toughness of 2000 times is reported for PVDF by grafting (chemical modification) the PVDF chains with amorphous polymer.[21] There remains a controversy in the scientific community regarding the structural issues (different phases) of fluoropolymer especially in the filled systems.[22,23] Moreover, the genesis of the different structures in the presence of specified dimension of filler is still unknown.

Polar β-phase is the determining factor for controlling the electronic properties as measured from piezoelectric coefficient, d_{33}. Stretching of film is one of the suitable methods to induce β-phase formation, but the brittleness in pure PVDF restricts the extent of the electronic phase. A maximum of 74% β-phase is reported through deconvolution of FTIR peaks for pure PVDF.[23] Improvement in toughness through hybrid formation in the presence of filler might help inducing more piezoelectric β-phase in fluoropolymers. Piezoelectric constant of PVDF, its copolymers, and hybrids with CNT is reported which depends on copolymer composition, filler concentration, and poling conditions.[24] There is no report of piezoelectric coefficient of PVDF in the presence of nanoclay where alteration in electronic structure is made possible with varying conditions.

In the present work, we report the super toughening phenomena induced by nanoparticle and process technology. The extent of piezoelectric phase of the nanohybrid has been enhanced to a significant level by controlled stretching under suitable condition. The literature reported long-standing ambiguity regarding phases, and melting behavior developed in the presence of nanoparticle has been resolved completely, and we proposed an in-depth model/mechanism of crystallization in the filled system for the first time explaining the different phases arise during crystallization on top of two-dimensional filler based on interaction and thermodynamic stability. Finally, we demonstrate the increased piezoelectric coefficient using the developed greater extent of piezoelectric β-phase induced by process technology and nanoparticle.

2. EXPERIMENTAL SECTION

Materials. Poly(vinylidene fluoride) (PVDF; SOLEF 6008, M_w = 2.7×10^5, PDI = 2.1, MFI = 24 g/10 min at 230 °C under 5 kg load) was kindly supplied by Ausimont, Italy. Bis(hydroxyethyl)methyl tallow ammonium ion exchanged montmorillonite (Cloisite 30B; density 1.98 g/cm^3) was purchased from Southern Clay Inc. and was used as filler to prepare the nanohybrids of PVDF. Dimethylformamide (DMF spectroscopic grade, Merck) was used as solvent to prepare hybrids.

Nanohybrids Preparation. Melt intercalation and solution casting methods were used for preparing PVDF/clay nanohybrids. In the solution casting method, DMF (dimethylformamide) is used for

dx.doi.org/10.1021/ma400603h | Macromolecules 2013, 46, 5595–5603

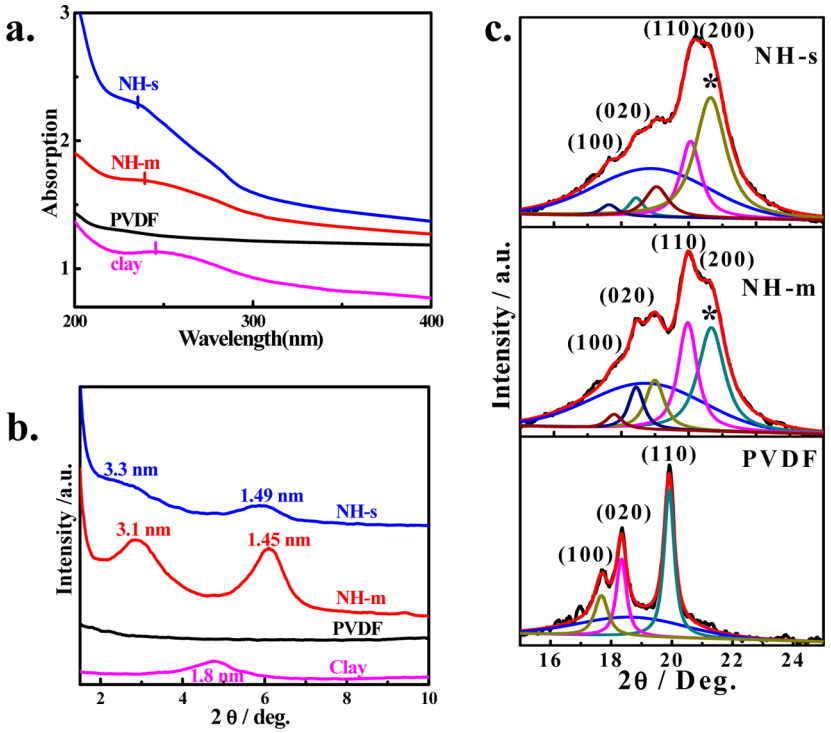

Figure 2. Variation in interaction. (a) UV–vis spectra of clay, pure PVDF, PVDF nanohybrid melt (NH-m), and solution (NH-s) processed. (b) Wide-angle XRD patterns of organically modified clay, pure PVDF, PVDF nanohybrid melt (NH-m), and solution casting (NH-s). Interplanar distance is indicated in nanometers. (c) Deconvolution of XRD patterns of pure PVDF, PVDF nanohybrid melt (NH-m), and solution casting (NH-s).

dissolving polymer followed by adding 4 wt % of nanoclay in the soluble polymer. Solvent was evaporated from the solution to make hybrid film and was kept in a vacuum oven for 48 h at a temperature of 80 °C to remove the trace amount of solvent from the film. In the melt intercalation method, twin-screw extruder (Thermo Scientific Haake MiniLab II) was used to carry out the extrusion process. Twelve grams of powdered PVDF and 480 mg of nanoclay were mixed in a high-speed homemade mixer for 2 h before putting the mixer in the extruder. The extrusion was carried out at a temperature of 205 °C for 10 min at a screw shear rate of 70 rpm. Henceforth, solution cast PVDF nanohybrid and melt extruded PVDF nanohybrids will be designated as NH-s and NH-m, respectively. We have studied different nanohybrids by varying the nanoclay concentration in PVDF matrix with 1, 2, 4, 6, 8, and 10 wt % and found 4 wt % nanohybrid as the optimum nanoclay content based on mechanical behavior. Therefore, most of the studies have been performed with nanohybrid having 4 wt % nanoclay. The details of the optimization studies have been reported in the Supporting Information.

Sample Preparation for Characterization. The injection molding technique was used to prepare the specimens for the measurement of mechanical properties using a Thermo Scientific Haake MiniJet II. The temperature of mold and barrel was maintained at 60 and 205 °C, respectively. A thin sheet sample (60 × 15 × 0.1 mm^3) for stretching in universal testing machine (UTM) at high temperature was prepared the through hot compression molding technique using a hot press compression molding machine (S.D. Instruments).

Characterization. *Tensile Testing.* An Instron 3369 was used to perform tensile testing at room temperature and at 90 °C at an elongation rate of 5 mm/min. Wedge action grips covered the wide parts of the specimen. The stress–strain data were recorded up to breaking point for samples and for various draw ratios separately. The samples were recovered after prefixed elongation. PVDF and its nanohybrid films with the thickness of ∼100 μm were also stretched unidirectional at a varying cross-head speed of 1, 5, 10, and 50 mm/min.

X-ray Diffraction. A Bruker AXS D8 Advance wide-angle X-ray diffractometer which was operating under a voltage of 40 kV and a current of 40 kA using Cu Kα radiation (λ = 0.154 nm) for recording X-ray diffraction (XRD) patterns of the pure polymer and its nanohybrids at a scan speed of 1°/min. XRD was also performed for stretched samples after recovered from tensile tests.

FTIR. A Nicolet 5700 instrument having a resolution of 4 cm^{-1} was used for performing FTIR analysis at room temperature in transmission mode. Thin samples of ∼40 μm are produced by compressing the polymer melt in between coverslips. Special care had been taken to produce air-bubble-free samples.

TEM. Transmission electron microscopy (TEM) was used to observe the nanoscale dispersion of nanoclay in the matrix polymer. TEM images were obtained using a Tecnai-G2-20 operated at an accelerating voltage of 200 kV. A thin layer was sectioned at −80 °C using a Leica ultracut UCT equipped with a diamond knife.

Scanning Electron Microscopy. SEM was used for investigating the surface morphology of pure PVDF and nanohybrids (melt and solution processed). Thin films, about 30 μm of the polymer and/or nanohybrids, were coated with Pd/Au alloy by means of an sputtering apparatus before observation in SEM (FESEM ZEISS SUPRA 40 instrument) operated at an accelerating voltage of 5 kV.

Differential Scanning Calorimetry (DSC). The heats of fusion of pure PVDF and its nanohybrids before and after stretching were determined via DSC using Mettler 832 at a scan rate of 10 °C min^{-1}. The peak temperature and enthalpy of fusion were measured from the endotherms using a computer attached with the instrument. The DSC was calibrated with indium before use.

Piezoelectric Coefficient. The piezoelectric response (d_{33}) of the poled samples was analyzed with a wide range d_{33}-meter (PM-300 of M/s Piezotest, UK). Poling was done by applying high voltage between the sides of the thin film in a silicon oil bath. The films were poled at electric field of 600 kV/cm at 85 °C for 10 min.

dx.doi.org/10.1021/ma400603h | *Macromolecules* 2013, 46, 5595–5603

3. RESULTS AND DISCUSSION

3.1. Process Induced Toughening. Process induced toughening behavior has been explored through stress−strain curves of PVDF and its nanohybrids with organically modified nanoclay prepared via melt (NH-m) and solution (NH-s) route (Figure 1a). The elongation at break increases for nanohybrids while it enhances significantly in solution processed hybrid, resulting improvement in toughness to 80% and 1100% for NH-m and NH-s, respectively, as compared to pure PVDF. In addition, the moduli increases to 755 and 865 MPa for NH-s and NH-m, respectively, against the 720 MPa of pure PVDF measured using the solution borne sample. The significant improvement in mechanical properties of nanohybrids derived from solution route has been explained from the homogeneous distribution and noteworthy smaller stack size of the nanoclay in the PVDF matrix (Figure 1b) in comparison to NH-m. Individual nanoclay platelets or fine dispersion have clearly been visible in NH-s having correlation length $\xi \sim 0.12$ μm in bright field TEM image against the thick tactoids in NH-m with $\xi \sim 0.45$ μm. The correlation length was measured from average distance between the two neighboring nanoclay disk/tactoids. Further, the relatively thinner and prominent needle-like crystallite morphology in NH-s (Figure 1c) supports the greater toughness vis-à-vis NH-m following the energy dissipation mechanism[15,25] of polymer under uniaxial stress field. The above toughening behavior has been performed with 4 wt % of nanoclay in nanohybrid (both for melt and solution route), and the particular concentration has been optimized from a series of nanoclay content (1−10 wt %) in nanohybrid based on the toughness, elongation at break, and modulus values as a function of nanoclay content and has been described in the beginning of the Supporting Information.

The residual stress is quite less in nanohybrids after stretching as evident from the squeezed film dimension (70% in NH-s and 47% in pure PVDF as compared to their respective original dimension) under heat treatment, confirming the fact that much of the energy has been spent to orient/rotate the nanoclay in nanohybrids and tiny needle-like crystallite help suppressing crack growth under stress field (Figure S1). On the other hand, large residual stress in pure PVDF wrinkles the specimen under heat treatment. It has to be mentioned that pure PVDF exhibits well-defined spherulitic morphology in its SEM surface image. The super toughened phenomena of NH-s as compared to NH-m and pure PVDF, as a result of superior dispersion, is further visualized from the blue-shift of UV absorption peak arising from intimate interaction of the nanoclay and PVDF. The absorption peak of nanoclay at 244 nm, due to olefinic double bond present in organic modifier, has shifted to 239 and 235.6 nm for NH-m and NH-s (Figure 2a), respectively, indicating greater interaction in NH-s, primarily due to fine dispersion.[16] The relative higher absorption of NH-s as compared to NH-m is presumably due to greater volume element of absorbing species due to fine dispersion even though the nanoclay content was kept similar in both the cases. It is needless to mention that PVDF does not have any absorption band in the energy range studied. As a consequence of greater interactions, the extent of intercalation of PVDF molecules inside the nanoclay galleries has been elevated in NH-s (3.3 nm) as compared to NH-m (3.0 nm) (Figure 2b). The higher intense peak at $2\theta \sim 6°$ (d-spacing 1.45 nm) is due to the epitaxial crystallization of PVDF[16] on the organically modified surface of nanoclay and will be discussed later. Apart from the dispersion and interactions, the extent of phase transformation to piezoelectric smaller crystallite (β-phase)[15] in the presence of nanoclay get enhanced in NH-s (35%) as compared to 25% in NH-m as observed through XRD deconvoluted peaks (Figure 2c). PVDF crystallizes in β form as obvious from the peak at $2\theta \sim 20.65°$ (200/110 planes) with its higher content in the presence of nanoclay in NH-s. Shifting of deconvoluted XRD peaks toward higher 2θ at 17.7° (110), 18.5° (020), and 20.0° (110) peak in NH-s in comparison to 17.68° (100), 18.3° (020), and 19.9° (110) peak position of α-phase, and the appearance of a new peak at $2\theta \sim 19.0°$ in nanohybrids indicates the formation of a metastable phase (distorted β- or γ-conformation) in the presence of nanoclay.[22] However, the α-phase and amorphous peak are present in nanohybrids though lesser in quantity. The development of FTIR absorption bands corresponds to β-phase appears with greater intensity in NH-s as compared to NH-m with gradual reduction of α-phase present in pure PVDF (Figure S2). It is noteworthy to mention that the β-phase formation in nanohybrids systematically increases with amount of nanoclay dispersed in PVDF as observed through respective higher intense peaks in XRD and FTIR studies. The systematic increase of melting point, as observed through differential scanning calorimetry, of 173.4, 174.8, and 178.0 °C for pure PVDF, NH-m, and NH-s, respectively, further supports the formation of additional β-phase in NH-s in comparison to NH-m (Figure S3) and will be discussed later.

The unusual toughening phenomena arising from the level of dispersion of nanoclay through processing leading to greater interaction and subsequent smaller crystallites of β-phase (as observed via SEM and XRD measurements) needs to be realized. Pure PVDF having well-developed spherulites exhibit brittle nature as usual,[26,27] while needle-like crystallites in hybrids, caused by the alteration in crystalline structure, are facile to orient/rotate along the stress field and, thereby, consume the energy which virtually suppress the crack growth translating the hybrid to be tougher[15] (Scheme 1). On the other hand, finer needle-like crystallites derived through solution route in NH-s are even better flippant as compared to NH-m toward orientation, causing super toughening of the hybrid prepared through the solution route. Usually, the better dispersion is expected in solution processed hybrid, and one may argue that just finer dispersion of nanoclay might cause super toughening phenomena. To circumvent the problem, we have compared the hybrids of a representative amorphous (PMMA) and a crystalline polymer (polyurethane, PU), where there is no change of structure in the presence of exactly the same nanoclay including its quantity (4 wt %). PMMA and polyurethane (PU) nanohybrids processed through solution route exhibit meager 20 and 26% higher toughness vis-à-vis their respective melt processed nanohybrids (Figure S4).

It is well-known that solution processed hybrids are better dispersed,[28] favoring slight improvement in toughness just because of dispersion in PMMA and PU systems. Surface induced crystallization of PVDF makes the system more frivolous and matrix friendly, leading to a huge 1100% improvement in toughness. It is worthy to mention that the plasticization effect of the solvent has been ruled out by drying the hybrids at reduced pressure at high temperature (80 °C), and eventually it does not play any role for solution borne PMMA or PU nanohybrids. Hence, structural change in nanohybrid has the major role for transforming into super toughened material in the presence of good dispersed nanoclay.

dx.doi.org/10.1021/ma400603h | Macromolecules 2013, 46, 5595−5603

Scheme 1. Schematic Representation of Unstretched (Spherulite) and Stretched PVDF (Spherulite Breakdown) and Schematic Representation for Orientation of Crystallite in PVDF Nanohybrid Melt (NH-m) and Solution Processed (NH-s) before and after Stretching[a]

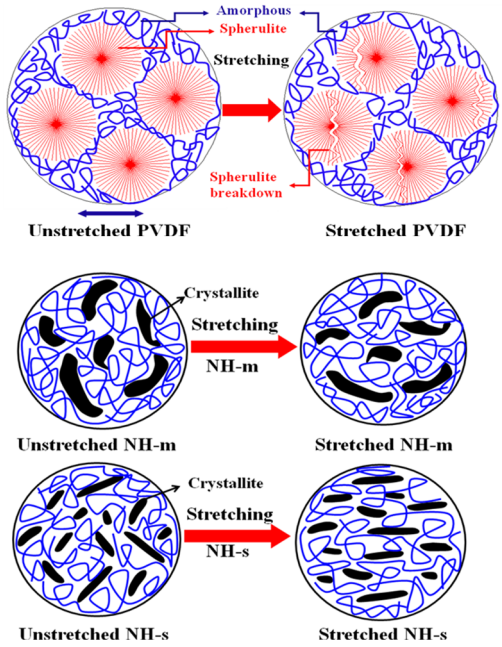

[a]The arrow shows the direction of stretching.

Two-dimensional disk-like nanoclay has a great advantage for structural alteration in the presence of heterogeneity over the zero-dimensional filler like silica[29] and titania,[30] where there is no change of structure at all, or one-dimensional filler like CNT/nanorod,[31] where there is a meager amount of induced β-phase due to dimensional constraints. Two-dimensional graphene sheets lead to the crystallization of predominantly α-phase PVDF with a very less β-phase,[32] as evident from the distinct spherulites in the hybrid, raises the requirement of compatibility and interaction of the filler with the matrix polymer. In this study, the organic modification on top of layered silicate increases the extent of interaction with polar PVDF. Suitable surface modification of nanoclay/2-D filler is the prime prerequisites to induce structural change as evident from predominant γ-phase crystallization of PVDF in the presence of unmodified montmorillonite, the inorganic constituent of the filler in this work.[22]

3.2. Induction of Piezoelectric Phase. As-prepared nanohybrids (NH-s) produce maximum 35% of β-phase fraction overall and is not sufficient to exhibit the piezoelectricity with that minimum piezoelectric phase embedded randomly in nonpolar crystalline (α-phase) and amorphous phase. In order to increase the β-phase content, the nanohybrids were stretched at higher temperature to favor the disentanglement under the stress field. The nanohybrid (NH-s) shows very high elongation at break (980%) as compared to pure PVDF (650%) (Figure 3). The structural analyses of pure PVDF exhibit gradual change of structure ($\alpha \rightarrow \beta$) with increasing draw ratio as evident from the appearance of peak at 20.4° due to (200/110) plane at draw ratio of 4.0 instead of 17.6°, 18.4°, and 19.9° peaks due to (100), (020), and (110) planes, respectively, of α-phase before stretching. In addition, the β-phase peak has shifted to higher angle for higher

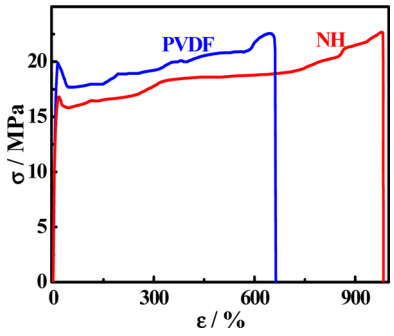

Figure 3. Stress−strain curves of thin film (120 μm thickness) at a temperature of 90 °C and draw rate of 5 mm/min for pure PVDF and PVDF nanohybrid solution cast (NH) showing the dramatic increase in elongation at break.

draw ratio (Figure 4a).[33] The β-phase fraction increases steadily in nanohybrid after stretching vis-à-vis as prepared nanohybrid.

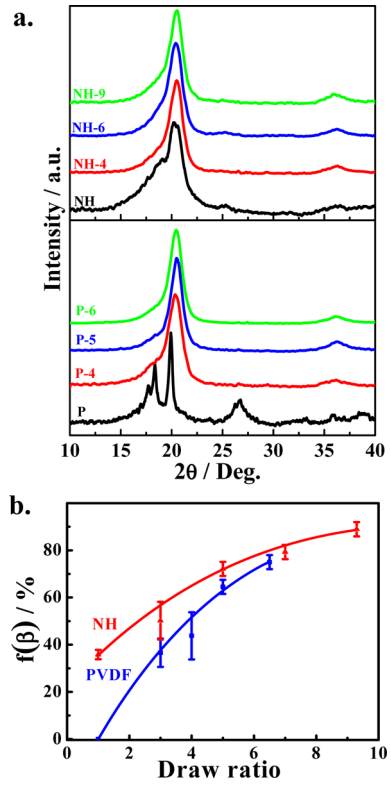

Figure 4. (a) XRD patterns of thin film of pure PVDF (P) and PVDF nanohybrid (NH) at different draw ratio; numeric terms after dash denote draw ratio. (b) β fraction, as calculated from the deconvoluted peaks, as a function of draw ratio of thin film for pure PVDF and its nanohybrid (NH) at the same condition as above.

The detailed analysis of the phase fraction has been presented in Figure S5 using deconvoluted diffractograms. Overall β-phase fraction increases gradually with draw ratio and attains a very high 90% for nanohybrid against 75% of pure PVDF in similar condition (Figure 4b), as calculated from the area under β-phase peak. The XRD patterns from 2θ = 30°−40° exhibit the formation of γ-phase along with β- phase in the presence of naoclay in PVDF (Figure S6). The structural development with draw ratio has also been substantiated through FTIR studies showing gradual higher intense β-peaks at 446, 512, 600, 745,

dx.doi.org/10.1021/ma400603h | Macromolecules 2013, 46, 5595−5603

837, 886, 1168, and 1274 cm^{-1} with increasing draw ratio in pure PVDF against pure α-phase peaks at 531, 764, 795, and 976 cm^{-1} before stretching (Figure 5).[22,34] On the contrary,

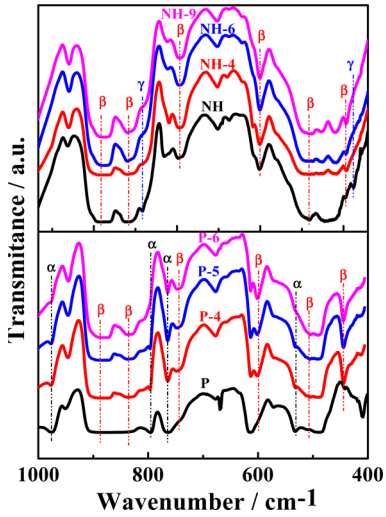

Figure 5. FTIR spectra of pure PVDF (P) and PVDF nanohybrid (NH) at different draw ratio showing the individuals α-, β-, and γ-phase peaks; numeric terms denote respective draw ratio of the sample.

nanohybrid shows all the above-mentioned β-peaks along with γ-phase peaks at 432, 811, and 1233 cm^{-1} before stretching.[22] Interestingly, the peak intensity of β-phase of NH-s systematically enhances with the disappearance of γ-phase with increasing draw ratio.

Figure S7 shows the other β- and γ-phase peaks at higher wavenumbers, confirming the presence of both the phases of as prepared samples and their respective development after stretching at various draw ratios. However, pure α-phase in PVDF converted into moderately high β-phase, while β- and γ-phase of NH transformed predominantly into β-phase after uniaxial elongation, leading to better piezoelectric hybrid material. It is to be mentioned that a small a small quantity of α-phase remain even at higher draw ratio as evident from a small trail in XRD peak and less intense α-peak in FTIR spectra.

3.3. Unique Melting in Filled System. There remains a unsolved issue of melting temperature (T_m) of PVDF specially in filled systems which shows higher T_m having certain β-phase against the literature reported lower T_m of pure β-PVDF (not in filled system) as compared to the T_m of α-PVDF. The DSC thermograms of pure PVDF stretched at various draw ratios exhibit gradual lowering of T_m with increasing draw ratio (Figure 6a) and clearly indicate the lower T_m of β-PVDF in unfilled system commensurate with the literature.[13,35] Higher temperature peak still exist for higher draw ratio (DR ~ 6) suggests few percentage of α-PVDF remains after stretching. On the other hand, nanohybrid (NH-s) shows T_m at 175 °C for β-phase and a high temperature peak at 178 °C, as evident from deconvoluted peak, before stretching presumably due to γ-phase.[13,35] Moreover, the main peak gradually decreases with increasing draw ratio, indicating transformation of either α- or amorphous phase to low melting β-phase. The high temperature peak assigned due to γ-phase at 178 °C gradually disappears at higher draw ratio as shown by vertical dotted line in Figure 6a, suggesting transformation of γ- to β-phase.[13] The changes in melting temperature as a function of draw ratio have been shown in Figure 6b, indicating gradual decreasing tendency at higher draw ratio. This decreasing order is presumably due to the formation of more β-phase (all-trans conformation) with stretching while the higher absolute values of nanohybrid vis-à-vis pure PVDF is due to certain fraction of γ-phase induced by nanoclay platelets as evident from FTIR and DSC measurements. The heat of fusion increases with draw ratio because of induced crystallinity upon stretching where amorphous phase has been transformed into β-crystalline phase while relatively less increment for nanohybrid as compared to pure PVDF occurs because of predominant $\alpha \rightarrow \beta$ and $\gamma \rightarrow \beta$ phase transformation as envisioned through

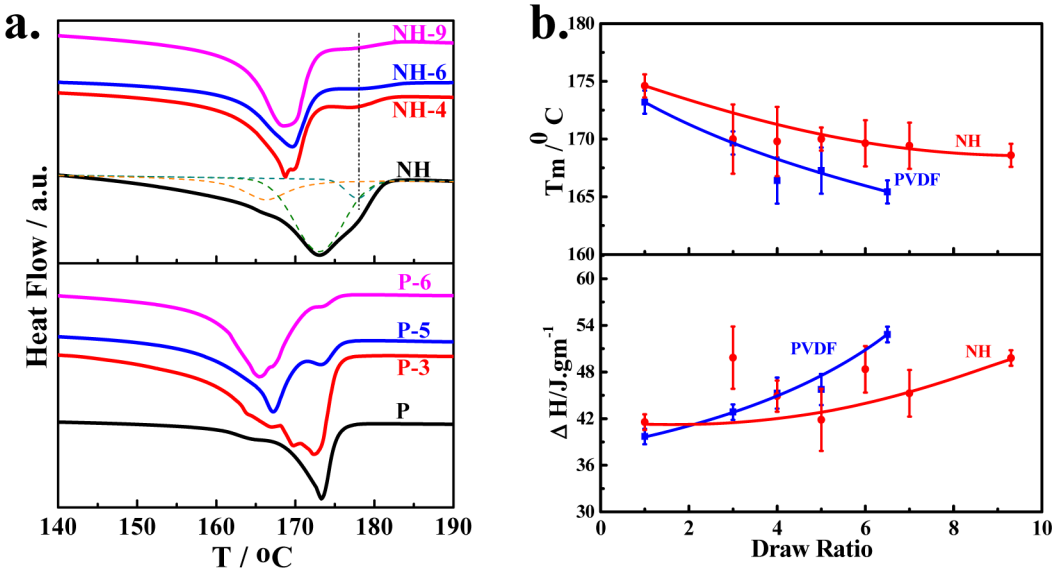

Figure 6. (a) DSC thermograms of pure PVDF (P) and PVDF nanohybrid (NH) at different draw ratio; numeric terms denote different draw ratio. (b) Melting temperature and heats of fusion as a function of draw ratio of thin film for pure PVDF and its nanohybrid (NH) at same condition as above.

dx.doi.org/10.1021/ma400603h | Macromolecules 2013, 46, 5595−5603

gradual decrease of α-phase and amorphous content with increasing draw ratio (Figure S8) and decreasing peak intensity in FTIR measurements (Figure 5). It has worth mentioning that the heat of fusion of α- and γ-phase is bit higher in comparison to β-phase.[31]

3.4. Typical Crystallization in Filled System. Now, it is clear that PVDF crystallizes in β- and γ-phases in the presence of nanoclay platelets against only α-phase crystallinity in unfilled PVDF, and the transformation into β-phase occurs upon stretching for both PVDF and its nanohybrids, while the extent of piezoelectric β-phase is maximum in nanohybrids as compared to pure PVDF. To investigate the origin of varying crystallization and super toughening mechanism in nanohybrids, we modeled the phenomena based on experimental evidence and has been presented in Scheme 2. As the PVDF

Scheme 2. Demonstration of the Structural Evolution on the Nanoclay Surface[a]

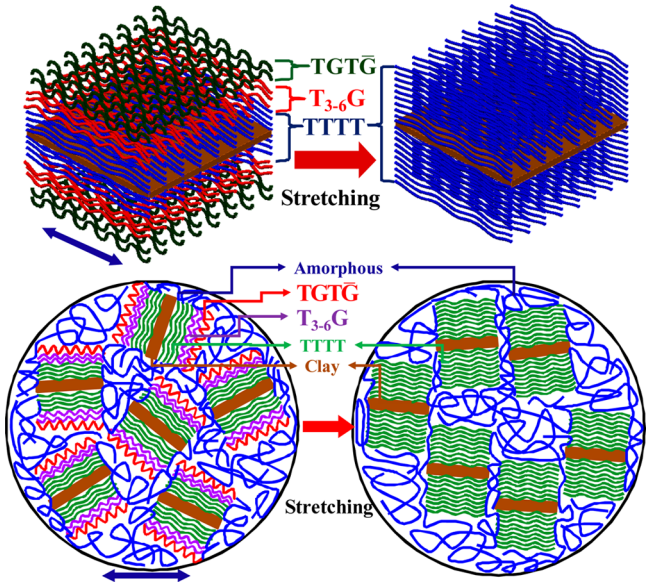

[a]Top part shows the schematic representation of structural change in PVDF nanohybrid solution casting (NH-s) before and after stretching on a single tactoid. First, second, and third layers on nanoclay surface are β-phase (TTTT), γ- or distorted γ-phase ($T_{3\text{-}6}G$), and α-phase ($TGT\bar{G}$), respectively, which converted into all β-phase after stretching (top right image). Bottom part shows overall structural change for couple of tactoids and their orientation under stress field.

crystallizes in β-phase just on top of nanoclay platelets[16] (Figure S7) γ-phase as evident from FTIR and DSC measurements and α-phase sufficiently away from the platelet, it is appropriate to consider that PVDF molecules crystallizes in all-trans conformation ($TTTT$) just on the vicinity of platelet surface, being strongly interactive nature of organically modified nanoclay and dipoles of PVDF as evident from gradual shifting to lower wavelength (blue-shift) of UV absorption peak in nanohybrids, presumably due to the subtle configurational changes of the organic modifier arising from intimate crystallization of PVDF in β-phase on top of organically modified platelets of nanoclay. After few layers of crystallization of PVDF molecules, the extent of interaction gets reduced, and there is a probability that change of conformation takes place from all-trans to T_3G or preferably $T_{3-6}G$ as the TG conformation is thermodynamically favorable having less energy,[13] while the PVDF molecules resides sufficiently away from nanoclay platelets experience lowest interaction and obviously crystallizes in thermodynamically most favored $TGT\bar{G}$ conformation of α-phase (−6.03 kcal/mol monomeric unit).[36] It is noteworthy to mention that there is no appreciable difference in intra- and intermolecular potential energy, consisting of van der Waals and electrostatic interactions, of α-form (−6.03 kcal/mol) and β-form (−5.73 kcal/mol) of PVDF in unfilled system.[36] But, the electrostatic interaction, which is ∼−0.19 kcal/mol monomeric unit in intermolecular interaction, considerably enhanced in filled system where there exist significant interaction arising from the dipoles of filler and polymer chain.[37] Therefore, the overall potential energy of β-phase in nanohybrid is lower (>−6.03 kcal/mol) than that of α-phase leading to crystallization of β-phase on top of nanoclay layers. The crystallization of γ-phase is favored after few layers of polymer chain in β-conformation on the nanoclay layers, where the electrostatic interaction is going to be lowered being apart from the nanoclay layers leading to TG conformation because of energy consideration. Hence, based on the relative interactions, the PVDF molecules crystallize on the surface of the nanoclay platelets in $TTTT$ (β-phase) and then $T_{3-6}G$ (a kind of γ-phase) and on top of them $TGT\bar{G}$ (α-phase) and ultimately create a crystalline island type of structure in nanometer dimension surrounding a two-dimensional platelet at the center. It is worthy to mention that one-dimensional CNT or two-dimensional graphene lacks this unique crystallization because of spatial constraints and insufficient interaction, respectively.[31,32] Moreover, those tiny crystalline islands are surrounded by amorphous polymer molecules situated at random in as-prepared nanohybrid and can orient/rotate easily during stretching (Scheme 2, bottom part) ultimately make the system super toughened by energy dissipation mechanism as discussed earlier. Further, the intermediate states ($T_{3-6}G$) and $TGT\bar{G}$ within an island convert into tiny β-phase which makes it even tougher and more piezoelectric (right bottom parts of the Scheme 2).

3.5. Induced Piezoelectricity. The structural improvement upon processing and nanoparticle has been demonstrated on piezoelectricity by measuring the piezoelectric coefficient (d_{33}) after poling the nanohybrids and has been compared with respect to pure PVDF. The piezoelectric coefficient is measured before and after stretching of poled PVDF and nanohybrids (Figure 7) with a representative draw ratio of 6.0. The value of

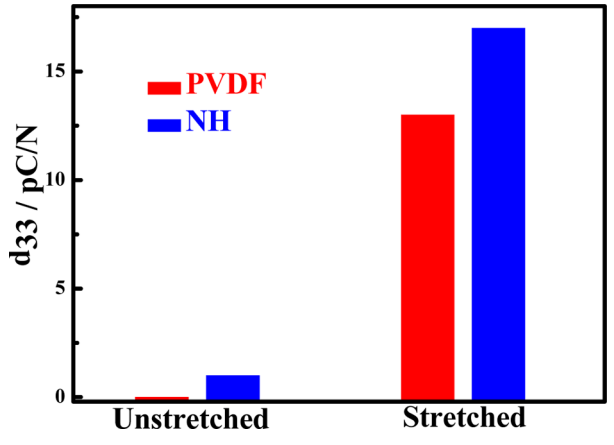

Figure 7. Bar diagram showing piezoelectric coefficient of PVDF and NH before and after stretching.

dx.doi.org/10.1021/ma400603h | Macromolecules 2013, 46, 5595−5603

d_{33} of unstretched nanohybrid is 1 pC/N in comparison to 0.1 value for PVDF before stretching indicate slight improvement in piezoelectricity due nucleation of ~35% of β-phase in the presence of nanoclay. A much higher d_{33} value in NH (17 pC/N) is measured against PVDF (13 pC/N) at a draw ratio of 6, which indicates the significant generation of piezoelectricity after stretching primarily due to enhanced β-phase as discussed in the previous sections (Figure 4b). The relatively higher d_{33} for nanohybrid is due to greater extent of β-phase generated in the presence of nanoclay. Similar improvement in d_{33} has been observed with MWCNT (multiwalled carbon nanotube) but at extreme poling condition of 100 °C at 1.5 MV cm^{-1} against our moderately soft poling state of 600 kV cm^{-1} at 85 °C.[38] The copolymer of PVDF[39] or polar γ-phase[40] exhibits much lower d_{33} value, signifying the high piezoelectricity of stretched PVDF especially in nanohybrid suitable for electromechanical devices. Hence, the generation of piezoelectric β-phase up to 90% has been reported using nanoparticle and process induced phenomena with shading the light on the exceptional crystallization behavior on top of two-dimensional nanoclay demonstrating high piezoelectric coefficient with super toughening behavior.

4. CONCLUSION

The nanohybrids of PVDF have been prepared through melt extrusion and the solution route. The super toughening phenomenon (1100%) with overall improvement in mechanical properties has been demonstrated for solution processed sample as compared to pure PVDF and melt processed nanohybrid. The unusual toughening behavior of solution processed nanohybrid over pure PVDF and melt processed nanohybrid has been explained from the greater alteration of structure ($\alpha/\gamma \rightarrow \beta$) with needle-like crystallite in the presence of nanoclay. A finer dispersion of nanoclay leads to greater interaction, as evident from relatively higher blue-shift in UV absorption, and directs the favorable induced structural and morphological changes. The unique crystallization mechanism in the filled system has been revealed showing β-phase on top of nanoclay platelets due to stronger interaction, and with increasing distance all-trans conformation has been changed to T_3G or distorted γ-form and ultimately converted to $TGT\bar{G}$ with further increasing distance from nanoclay layers obeying the energy consideration. The extent of piezoelectric β-phase has been enhanced in nanohybrid to 90% against 75% in pure PVDF after stretching at higher temperature to favor the disentanglement and has been confirmed through XRD, FTIR, and DSC measurements. The relative enhancement of piezoelectric β-phase in nanohybrid has been reflected in higher piezoelectric coefficient as compared to pure PVDF, leading to the creation of super toughened piezoelectric hybrid material.

■ ASSOCIATED CONTENT

Supporting Information

Experimental details; Figures S1−S8. This material is available free of charge via the Internet at http://pubs.acs.org.

■ AUTHOR INFORMATION

Corresponding Author

*E-mail: pmaiti.mst@itbhu.ac.in (P.M.).

Notes

The authors declare no competing financial interest.

■ ACKNOWLEDGMENTS

The authors acknowledge Dr. D. K. Avasthi and Mr. Pawan K. Kulriya for assisting in XRD studies. The kind supply of PVDF samples by Ausimont, Italy, is highly acknowledged. Vimal K. Tiwari acknowledges the award of Senior Research Fellowship of CSIR, India.

■ REFERENCES

(1) Lee, C. S.; Joo, J.; Han, S.; Koh, S. K. *Appl. Phys. Lett.* **2004**, *85* (10), 1841.
(2) Khanna, P. K.; Hornbostel, B.; Grimme, R.; Schaefer, W.; Dorner, J. *Mater. Chem. Phys.* **2004**, *87* (1), 173.
(3) Valentini, R. F.; Vargo, T. G.; Gardella, J. A.; Aebischer, P. *J. Biomater. Sci., Polym. Ed.* **1993**, *5*, 13.
(4) Tashiro, K.; Tadokoro, H.; Kobayashi, M. *Ferroelectrics* **1981**, *32*, 167.
(5) Adem, E.; Rickards, J.; Burillo, G.; Avalos-Borja, M. *Radiat. Phys. Chem.* **1999**, *54*, 637.
(6) Heymans, N.; El Mohajir, B.-E. *Polymer* **2001**, *42*, 5661.
(7) McGrath, J. C.; Ward, I. M. *Polymer* **1980**, *21*, 855.
(8) Scheinbeim, J.; Nakafuku, C.; Newman, B. A.; Pae, K. D. *J. Appl. Phys.* **1979**, *50*, 4399.
(9) Wang, J.; Li, H.; Liu, J.; Duan, Y.; Jiang, S.; Yan, S. *J. Am. Chem.. Soc.* **2003**, *125*, 1496.
(10) Kobayashi, M.; Tashiro, K.; Tadokoro, H. *Macromolecules* **1975**, *8*, 158.
(11) Lovinger, A. J. *Polymer* **1981**, *22*, 412.
(12) Prest, W. M.; Luca, D. J., Jr. *J. Appl. Phys.* **1975**, *46* (10), 4136.
(13) Prest, W. M.; Luca, D. J., Jr. *J. Appl. Phys.* **1978**, *49* (10), 5042.
(14) Priya, L.; Jog, J. P. *J. Polym. Sci., Part B: Polym. Phys.* **2002**, *40*, 1682.
(15) Shah, D.; Maiti, P.; Gunn, E.; Schmidt, D. F.; Jiang, D. D.; Batt, C. A.; Giannelis, E. P. *Adv. Mater.* **2004**, *16* (14), 1173.
(16) Tiwari, V. K.; Shripathi, T.; Lalla, N. P.; Maiti, P. *Nanoscale* **2012**, *4*, 167.
(17) Sheth, J.; Kumar, D.; Tiwari, V. K.; Maiti, P. *J. Mater. Res.* **2012**, *27* (14), 1838.
(18) Layek, R. K.; Samanta, S.; Chatterjee, D. P.; Nandi, A. K. *Polymer* **2010**, *51*, 5846.
(19) Kang, S. J.; Park, Y. J.; Bae, I.; Kim, K. J.; Kim, H.-C.; Bauer, S.; Thomas, E. L.; Park, C. *Adv. Funct. Mater.* **2009**, *19*, 2812.
(20) Li, M.; Stingelin, N.; Michels, J. J.; Spijkman, M.-J.; Asadi, K.; Feldman, K.; Blom, P. W. M.; de Leeuw, D. M. *Macromolecules* **2012**, *45*, 7477.
(21) Samanta, S.; Chatterjee, D. P.; Manna, S.; Mandal, A.; Garai, A.; Nandi, A. K. *Macromolecules* **2009**, *42*, 3112.
(22) Lopes, A. C.; Costa, C. M.; Tavares, C. J.; Neves, I. C.; Mendez, S. L. *J. Phys. Chem. C* **2011**, *115*, 18076.
(23) Liu, Y. L.; Li, Y.; Xu, J. T.; Fan, Z. Q. *ACS Appl. Mater. Interfaces* **2010**, *2* (6), 1759.
(24) Salimi, A. *Polym. Test.* **2003**, *22*, 699.
(25) Shah, D.; Maiti, P.; Jiang, D. D.; C. Batt, A.; Giannelis, E. P. *Adv. Mater.* **2005**, *17*, 525.
(26) Tiwari, V. K.; Kulriya, P. K.; Avasthi, D. K.; Maiti, P. *ACS Appl. Mater. Interfaces* **2009**, *1* (2), 311.
(27) Tiwari, V. K.; Kulriya, P. K.; Avasthi, D. K.; Maiti, P. *J. Phys. Chem. B* **2009**, *113*, 11632.
(28) Li, Y.; Shimizu, H. *Macromolecules* **2008**, *41*, 5339.
(29) Kim, J. W.; Cho, W. J.; Ha, C. S. *J. Polym. Sci., Part B: Polym. Phys.* **2002**, *40*, 19.
(30) Li, J.; Seok, S.; Chu, B.; Dogan, F.; Zhang, Q.; Wang, Q. *Adv. Mater.* **2009**, *21*, 217.
(31) Manna, S.; Nandi, A. K. *J. Phys. Chem. C* **2007**, *111*, 14670.
(32) Yu, J.; Jiang, P.; Wu, C.; Wang, L.; Wu, X. *Polym. Compos.* **2011**, *32*, 1483.
(33) Hasegawa, R.; Takahashi, Y.; Chatani, Y.; Tadokoro, H. *Polym. J.* **1972**, *3* (5), 600.

(34) Mendez, S. L.; Mano, J. F.; Costa, A. M.; Schmidt, V. H. *J. Macromol. Sci., Phys.* **2001**, *B40* (3&4), 517.
(35) Tashiro, K.; Kobayashi, M.; Tadokoro, H. *Macromolecules* **1981**, *14*, 1757.
(36) Hasegawa, R.; Kobayashi, M.; Tadokoro, H. *Polym. J.* **1972**, *3* (5), 591.
(37) Podsiadlo, P.; Kaushik, A. K.; Arruda, E. M.; Waas, A. M.; Shim, B. S.; Xu, J.; Nandivada, H.; Pumplin, B. G.; Lahann, J.; Ramamoorthy, A.; Kotov, N. A. *Science* **2007**, *318*, 80.
(38) Kim, G. H.; Hong, S. M.; Seo, Y. *Phys. Chem. Chem. Phys.* **2009**, *11*, 10506.
(39) He, X.; Yao, K.; Gan, B. K. *J. Appl. Phys.* **2005**, *97*, 084101.
(40) Lopes, A. C.; Costa, C. M.; Tavares, C. J.; Neves, I. C.; Lanceros-Mendez, S. *J. Phys. Chem. C* **2011**, *115*, 18076.